Biomedical Optics EXPRESS

Method of detecting tissue contact for fiber-optic probes to automate data acquisition without hardware modification

Sarah Ruderman,[1,*] Scott Mueller,[2] Andrew Gomes,[1] Jeremy Rogers[1] and Vadim Backman[1]

[1]*Department of Biomedical Engineering, Northwestern University, 2145 Sheridan Road, Evanston, IL 60208, USA*

[2]*American BioOptics, 1801 Maple Ave Evanston, IL 60201, USA*

[*]*ruderman@u.northwestern.edu*

Abstract: We present a novel algorithm to detect contact with tissue and automate data acquisition. Contact fiber-optic probe systems are useful in noninvasive applications and real-time analysis of tissue properties. However, applications of these technologies are limited to procedures with visualization to ensure probe-tissue contact and individual user techniques can introduce variability. The software design exploits the system previously designed by our group as an optical method to automatically detect tissue contact and trigger acquisition. This method detected tissue contact with 91% accuracy, detected removal from tissue with 83% accuracy and reduced user variability by $>$ 8%. Without the need for additional hardware, this software algorithm can easily integrate into any fiber-optic system and expands applications where visualization is difficult.

OCIS codes: (170.1610) Clinical applications; (060.2310) Fiber optics; (120.1880) Detection; (230.3120) Integrated optics devices; (170.6510) Spectroscopy, tissue diagnostics.

References and links

1. M. Keshtgar, D. Chicken, M. Austwick, S. Somasundaram, C. Mosse, Y. Zhu, I. Bigio, and S. Bown, "Optical scanning for rapid intraoperative diagnosis of sentinel node metastases in breast cancer," Brit. J. Surg. **97**, 1232–1239 (2010).
2. R. L. van Veen, A. Amelink, M. Menke-Pluymers, C. van der Pol, and H. J. Sterenborg, "Optical biopsy of breast tissue using differential path-length spectroscopy," Phys. Med. Biol. **50**, 2573 (2005).
3. J. R. Mourant, T. M. Powers, T. J. Bocklage, H. M. Greene, M. H. Dorin, A. G. Waxman, M. M. Zsemlye, and H. O. Smith, "In-vivo light scattering for the detection of cancerous and precancerous lesions of the cervix," Appl. Opt. **48**, D26–D35 (2009).
4. Y. Zhu, N. G. Terry, and A. Wax, "Angle-resolved low-coherence interferometry: an optical biopsy technique for clinical detection of dysplasia in barrett's esophagus," Expert Rev. Gastroenterol. Hepatol. **6**, 37–41 (2012).
5. N. Thekkek, S. Anandasabapathy, and R. Richards-Kortum, "Optical molecular imaging for detection of barretts associated neoplasia," World J. Gastroentero. **17**, 53 (2011).
6. H. K. Roy, A. Gomes, V. Turzhitsky, M. J. Goldberg, J. Rogers, S. Ruderman, K. L. Young, A. Kromine, R. E. Brand, M. Jameel, P. Vakil, N. Hasabou, and V. Backman, "Spectroscopic microvascular blood detection from the endoscopically normal colonic mucosa: biomarker for neoplasia risk," Gastroenterology **135**, 1069–1078 (2008).
7. L. Lim, B. Nichols, N. Rajaram, and J. W. Tunnell, "Probe pressure effects on human skin diffuse reflectance and fluorescence spectroscopy measurements," J. Biomed. Opt. **16**, 011012 (2011).
8. Y. Ti and W. C. Lin, "Effects of probe contact pressure on in vivo optical spectroscopy," Opt. Express **16**, 4250–4262 (2008).

#192160 - $15.00 USD Received 13 Jun 2013; revised 15 Jul 2013; accepted 17 Jul 2013; published 23 Jul 2013

9. V. T.C. Chang, D. Merisier, B. Yu, D. K. Walmer, and N. Ramanujam, "Towards a field-compatible optical spectroscopic device for cervical cancer screening in resource-limited settings: effects of calibration and pressure," Opt. Express **19**, 17908–17924 (2011).
10. R. Reif, M. S. Amorosino, K. W. Calabro, O. AAmar, S. K. Singh, and I. J. Bigio, "Analysis of changes in reflectance measurements on biological tissues subjected to different probe pressures," J. Biomed. Opt. **13**, 010502 (2008).
11. S. Ruderman, A. J. Gomes, V. Stoyneva, J. D. Rogers, A. J. Fought, B. D. Jovanovic, and V. Backman, "Analysis of pressure, angle and temporal effects on tissue optical properties from polarization-gated spectroscopic probe measurements," Biomed. Opt. Express **1**, 489 (2010).
12. M. Lu, J. Xiong, and T. Cui, "A flexible tri-axis contact force sensor for tubular medical device applications," J. Micromech. Microeng. **21**, 035004 (2011).
13. K. Yokoyama, H. Nakagawa, D. C. Shah, H. Lambert, G. Leo, N. Aeby, A. Ikeda, J. V. Pitha, T. Sharma, R. Lazzara *et al.* "Novel contact force sensor incorporated in irrigated radiofrequency ablation catheter predicts lesion size and incidence of steam pop and thrombusclinical perspective," Circ. Arrhythm. Electrophysiol. **1**, 354–362 (2008).
14. A. Chouinard, "Linear gap displacement transducer sheds light on proximity sensing," Sensors Mag. **18**, 18 (2001).
15. T. Y. Lin, P. C. P. Chao, W. D. Chen, and C. H. Tsai, "A novel 3-d optical proximity sensor panel and its readout circuit," IEEE Sensors. 108–113 (2010).
16. R. H. Kim, D. H. Kim, J. Xiao, B. H. Kim, S. I. Park, B. Panilaitis, R. Ghaffari, J. Yao, M. Li, Z. Liu, V. Malyarchuk, D. G. Kim, A. P. Le, R. G. Nuzzo, D. L. Kaplan, F. G. Omenetto, Y. Huang, Z. Kang, and J. A. Rogers, "Waterproof AlInGaP optoelectronics on stretchable substrates with applications in biomedicine and robotics," Nat. Mater. **9**, 929–937 (2010).
17. L. Bürgi, R. Pfeiffer, M. Mücklich, P. Metzler, M. Kiy, and C. Winnewisser, "Optical proximity and touch sensors based on monolithically integrated polymer photodiodes and polymer leds," Org. Electron. **7**, 114–120 (2006).
18. E. Cibula and D. Donlagic, "Miniature fiber-optic pressure sensor with a polymer diaphragm," App. Opt. **44**, 2736–2744 (2005).
19. A. Nath, K. Rivoire, S. Chang, D. Cox, E. N. Atkinson, M. Follen, and R. Richards-Kortum, "Effect of probe pressure on cervical fluorescence spectroscopy measurements," J. Biomed. Opt. **9**, 523–533 (2004).
20. V. M. Turzhitsky, A. J. Gomes, Y. L. Kim, Y. Liu, A. Kromine, J. D. Rogers, M. Jameel, H. K. Roy, and V. Backman, "Measuring mucosal blood supply in-vivo with a polarization-gating probe," App. Opt. **47**, 6046–6057 (2008).
21. E. Rodriguez-Diaz, C. S. Huang, A. Sharma, L. I. Jepeal, I. J. Bigio, and S. K. Singh, "Optical sensing of field carcinogenesis in colonic mucosa using elastic-scattering spectroscopy," Gastroenterology **140**, S–751 (2011).
22. H. K. Roy, N. N. Mutyal, A. Radosevich, S. Bajaj, J. Van Dam, V. J. Konda, J. D. Rogers, S. Upadhye, M. J. Goldberg, and V. Backman, "Development and clinical performance of a novel low coherence enhanced backscattering spectroscopy (lebs) fiberoptic probe for duodenal sensing of pancreatic cancer risk," Gastroenterology **142**, S–207 (2012).
23. J. M. Yamal, D. D. Cox, E. N. Atkinson, C. MacAulay, R. Price, and M. Follen, "Repeatability of tissue fluorescence measurements for the detection of cervical intraepithelial neoplasia," Biomed. Opt. Express **1**, 641 (2010).

1. Introduction

Numerous groups use fiber-optic probes that exploit scattering, absorption and fluorescence of tissue for diagnostic capabilities, including breast [1, 2], cervical [3], esophageal [4, 5] and colon [6], among others. The nature of these technologies require the fiber-optic probe maintain contact with the target tissue for data acquisition. This limits applications to procedures with direct visualization of the target tissue (i.e. endoscopic use) or potential inaccuracies in measurements where contact is difficult to confirm visually (i.e. laparoscopic procedures). Additionally, there is concern that pressure applied by the probe to the tissue affects the physiological parameters measured. Increasing probe pressure was shown to decrease blood volume and oxygen saturation over extended exposure times in diffuse reflectance and fluorescence spectroscopy on the forehead and neck of human skin [7]. In diffuse reflectance spectroscopy, increasing probe pressure caused spectral profile alterations of rat heart and liver tissue measurements [8], decreased hemoglobin absorption and increased scattering on cervical tissue [9], and increased the reduced scattering coefficient on mouse thigh muscle [10]. Our group previously reported similar changes in hemoglobin concentration and reduced scattering coefficient with increased

#192160 - $15.00 USD Received 13 Jun 2013; revised 15 Jul 2013; accepted 17 Jul 2013; published 23 Jul 2013

probe pressure, as well as a decrease in oxygenation as the length of contact time between the probe and tissue increased [11]. Variations in optical measurements due to potential user effects of applied pressure and contact time can directly impact the diagnostic accuracy of the device. Integrating a method that detects contact between the fiber-optic probe and target tissue and automating data acquisition can mitigate these effects. Accurately detecting tissue contact can expand the use of fiber-optic probe devices beyond endoscopic procedures to blind insertion in easily accessible tissues (i.e. rectum and cervix) for diagnostic and screening applications.

Sensors have been developed that can help indicate contact between the sensor and an object. The sensors most applicable to fiber-optic probes generally fall into one of three classes: contact, proximity, or pressure sensors. A capacitive, tri-axis contact force sensor was fabricated that can be inserted into small diameter, tubular medical devices. The capacitance change between two SU-8 plates indicates the amplitude and direction of the applied force on the tip [12]. Another contact force sensor was incorporated into the distal part of a radio frequency ablation catheter. The applied pressure, or contact force, deforms a fiber Bragg grating in three optical fibers, resulting in a change in the reflected wavelength [13]. Similarly, a probe with three concentric fiber rings illuminates an object from the center ring and uses the ratio of reflected light in the outer two rings to determine the distance from the probe tip to the object [14]. Another optical proximity sensor placed light-emitting-diodes (LEDs) on an array of polymer photo-detectors (PPDs). The reflected light from an object is converted into an electrical signal proportional to the distance between the object and sensor array [15]. This same concept was adapted to create small, flexible optical-proximity-sensor tapes that can be conformed on curved surfaces and made waterproof for surgery, implants or other biomedical applications [16]. A dual mode sensor was designed with this LED/PPD array for proximity or contact. The proximity mode again uses reflected light to measure distance, where the contact mode relies on a change in effective refractive index when an object touches the sensor [17]. A miniature pressure sensor was created with a thin polymer diaphragm positioned inside the hollow end of an optical fiber. The applied pressure is measured by deflection in the diaphragm [18]. Alternatively, a spring-loaded device could be mounted at the proximal end of a fiber optic probe to monitor applied pressure [19]. Other designs methods could integrate capacitive, inductive, piezoelectric, piezoresistive or multi-component elements into the fiber-optic probes.

All these techniques require engineering and changing the probe design, which add complexity and cost to our probes. There may be a software solution to create an automated contact sensor without any hardware modification. An optical method could be the most economical and viable solution for biomedical applications already using fiber-optic probe systems for tissue analysis. Our goal was to develop an algorithm that used the current components of our system in order to avoid redesigning the proximal tip of the probe with additional hardware or mechanical components. In this paper, we present the software algorithm to detect contact with tissue, parameters that can be modified for other fiber-optic systems, and an in-vivo evaluation of the algorithm performance. To the best of our knowledge, our work demonstrates the first automated method integrated into a fiber-optic probe that accurately detects contact with tissue and reliably automates data acquisition, even when visualization is not available.

2. Background

We previously developed an endoscopically-compatible fiber-optic probe for in-vivo polarization-gating spectroscopy (PGS) analysis during colonoscopy [20]. The probe is $2.5mm$ in diameter and consists of three $200\mu m$-core diameter fibers: one for illumination of tissue, coupled to a white light LED (WT&T); and the other two for collection of co-polarized and cross-polarized signals, coupled to individual spectrometers (Ocean Optics, USB2000). A computer interface allows users to control data acquisition. The schematic is shown in Fig. 1.

#192160 - $15.00 USD Received 13 Jun 2013; revised 15 Jul 2013; accepted 17 Jul 2013; published 23 Jul 2013

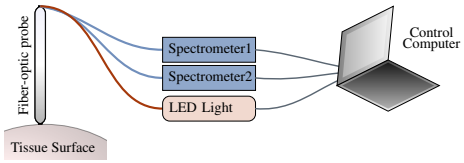

Fig. 1. Schematic diagram of polarization-gating probe and system.

In a previous study [11], we demonstrated that firm pressure impacts the data collected and needs to be addressed in the clinical setting. We showed that when firm pressure (estimated at $0.15-0.2N/mm^2$) is applied to the probe, the measured oxygenation of the tissue site continually decreases during an interval of 30 seconds. If gentle pressure (estimated at $0.009-0.012N/mm^2$) is maintained throughout probe contact with tissue, no significant change is observed in oxygenation (Fig. 2 adapted from Ref. [11]). Although the estimated pressures for each user in this study were subject to interpretation, in a clinical setting, the pressure applied to the probe through an endoscope is harder to assess and can introduce a source of variability among endoscopists. There were no significant changes between gentle and firm pressures within the first 5 seconds following the initial measurement. In most research applications, a delay greater than 5 seconds is likely between the moment the physician places the probe in contact with tissue and communicates this to the user, who then initiates data acquisition. Automating measurements in a reliable manner can decrease temporal variability because it eliminates the need of a required action from the user and ensures any delay between tissue contact and data acquisition is consistent.

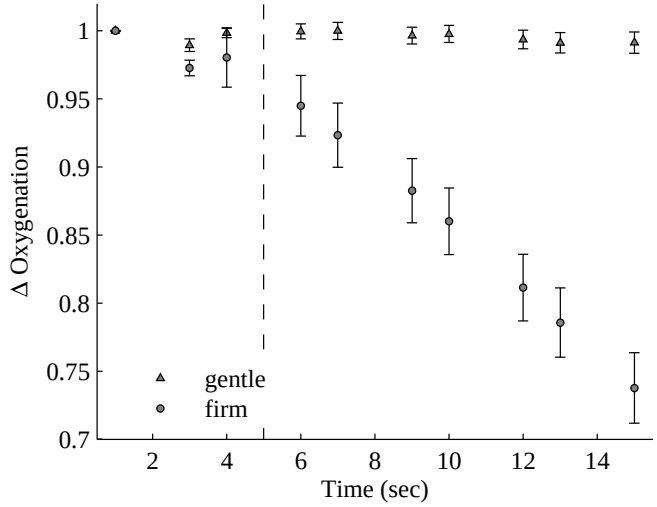

Fig. 2. Temporal change in oxygenation with applied pressure. Oxygenation continues to decrease during the 15 seconds when pressure is applied to the probe. For measurements within the first 5 seconds (left of the dashed line), there is no significant change at either pressure. Oxygenation measurements were normalized to the first measurement in the sequence, corresponding to initial probe contact. Either gentle or firm pressure was applied consistently throughout the measurement sequence. Data and graph adapted from Ref. [11]

Potential solutions to reduce variability include: (1) a standardized protocol to maintain gentle pressure between the probe tip and tissue; (2) integrating a sensor to control the pressure applied to the probe tip; and (3) control the start time of data acquisition to minimize any delay

#192160 - $15.00 USD Received 13 Jun 2013; revised 15 Jul 2013; accepted 17 Jul 2013; published 23 Jul 2013

after initial probe-tissue contact. These do not addresses the clinical need to detect probe-tissue contact in situations with limited or no visualization of the target tissue. Thus, the optimal solution is a robust mechanism to both detect probe-tissue contact and automatically trigger the start of data acquisition. A software algorithm would be a simple addition to current fiber-optic systems. By manipulating the light source and spectrometers/detectors, this algorithm alleviates the need to redesign fiber-optic probes with hardware modifications which would add complexity and cost.

3. Methods

The flow chart in Fig. 3 outlines the software algorithm developed, from the user initiating the system to the completion of a sequence of tissue measurements. A state machine is used to drive the contact detection algorithm which separates the program into narrowly defined tasks (states and state transitions). Alternate programming constructs could be substituted, such as selection statements or iteration loops. The state machine provides the sequencing of the steps necessary to acquire the reflected light readings for both the contact detection and the tissue physiological measurements. This design includes the following states: setup, configuring spectrometers for contact detection, acquiring contact detection, evaluating contact detection, configuring spectrometers for tissue measurement, acquiring tissue measurement, evaluating tissue measurement, configuring spectrometers for probe retraction, acquiring probe retraction, evaluating probe retraction, and a complete state.

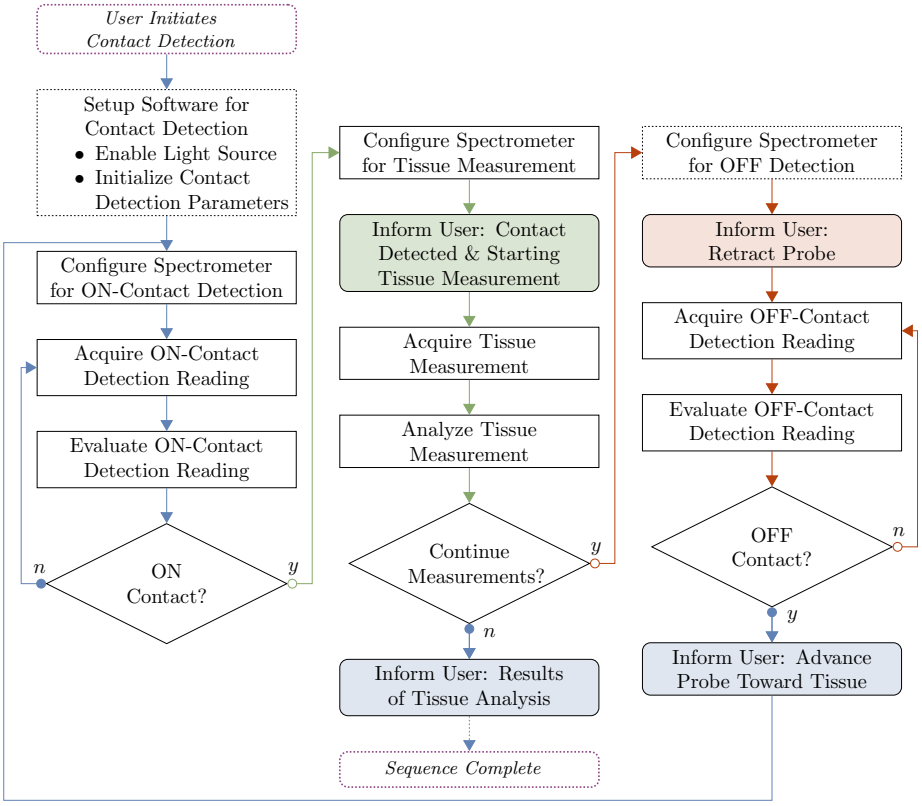

Fig. 3. Algorithm Flow Chart

The algorithm detects contact between the probe and tissue by continuously and rapidly

#192160 - $15.00 USD Received 13 Jun 2013; revised 15 Jul 2013; accepted 17 Jul 2013; published 23 Jul 2013

monitoring the reflected intensity from the tissue, then evaluating the data against predetermined criteria. To begin, the user initiates the system and the software enables the light source and configures the spectrometers for on contact detection parameters. The complete contact sequence to trigger data acquisition requires 5 consecutive readings at the optimal wavelength above the threshold with $< 3\%$ variability. This process takes approximately $850ms$, and the software then switches modes to acquire the tissue measurement. The contact parameters are discussed in detail below and include: (1) specific wavelength range (10 pixels around 525nm); (2) normalized threshold intensity ratio (above 0.08); (3) consistent threshold value (within 3% for 5 consecutive measurements); and (4) integration time (20ms).

We evaluated the reflected signal intensity as a function of distance from tissue to determine the optimal wavelength to indicate tissue proximity and contact. Figure 4 illustrates signal intensity for increasing distances from the tissue surface at 450nm, 525nm and 650nm. Using a single wavelength, instead of the full spectrum used in tissue analysis, reduced data transfer speeds. These wavelengths were selected for high signal output of our light source with lower hemoglobin absorption. For all wavelengths, as the probe approaches the tissue, the amount of reflected light increases. The large jump in signal intensity observed between 4mm and 2mm from the tissue surface can serve as an indicator of tissue proximity. Our previous study reported that the tissue properties measured by our system did not depend on the angle between the axis of the probe tip and tissue surface since good contact allows the tissue to conform to the probe tip [11]. When evaluating the angle between the probe and tip as a function of distance, angles as large as 45-60 degrees from normal to the tissue surface did not affect the reflected intensity. More extreme angles (i.e. probe tangential to tissue surface) cause fluctuations in reflected intensity that resembles the probe sliding along the tissue surface (discussed in Fig. 5). The wavelength range near 525nm remained the most consistent in tissue measurements with minimal interference from ambient light, such as from endoscope illumination.

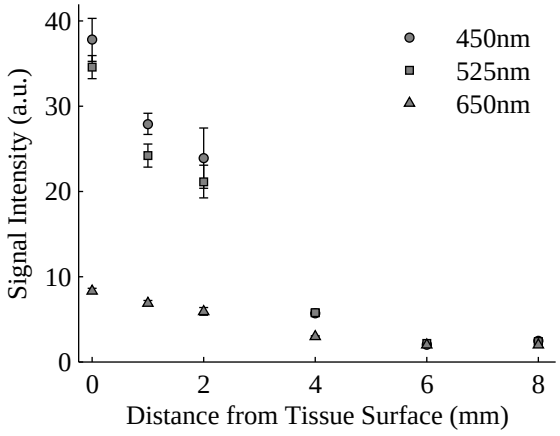

Fig. 4. Wavelength Range Optimization. Reflected intensity at distinct wavelengths to establish signal changes with proximity to tissue. Reflected intensity increases as fiber-optic probe approaches the tissue surface.

Next, the change in reflected intensity needs to be translated into a threshold for contact detection. Figure 5 represents the trend of the normalized reflected intensity as the probe is advanced into and out of contact with colon mucosa during a colonoscopy. The square wave nature of this trend suggests that discrete threshold values could be selected for ”ON”-contact and ”OFF”-contact. To account for system, probe and biological variability, the reflected tissue

#192160 - $15.00 USD Received 13 Jun 2013; revised 15 Jul 2013; accepted 17 Jul 2013; published 23 Jul 2013

intensity is normalized by a calibration measurement of a reflectance standard (SRS-99-010, Labsphere, Inc.) acquired immediately before in-vivo data collection.

After evaluating in-vivo data similar to that in Fig. 5 from more than 20 patients, we established threshold ratios (tissue/calibration) where ON-contact ≥ 0.08 and OFF-contact < 0.06. This ON-contact threshold detects when the probe is within $2mm$ of the tissue. The time required for the probe to travel the remaining distance and establish stable contact with the tissue is typically $< 100ms$. This is less than the time needed by the system software to setup for tissue measurement acquisition ($\sim 150ms$). The threshold values apply to our particular system components and can easily be adapted to account for the sensitivity of different spectrometers, as well as the transmission properties of different probes.

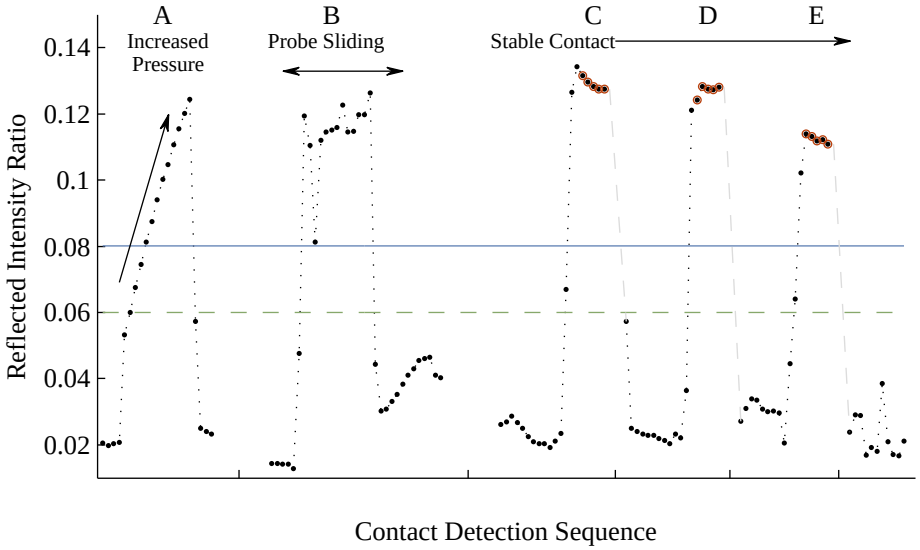

Fig. 5. Illustration of automated trigger sequence. Graph represents 3 isolated sequences when the probe was placed in contact with tissue. The first, labeled A, shows applying pressure to the probe continues to increase the reflected intensity. The second, labeled B, shows large variation in reflected intensity when the probe slides along tissue surface. Both cases have recordings above the ON-threshold with variability $> 3\%$ and therefore, do not trigger data acquisition. The last sequence, labeled C-E, is a continuous set of detection readings and red circles highlight the 5 consecutive readings required for stable contact. The dashed line after each set of red points indicate when a tissue measurement was triggered, the program switched modes to acquire and transfer data, and then resumed contact detection mode (avg $600ms$). Each point indicates the recorded reflected intensity and the sampling interval is 170ms for points connected by the dotted line. Ticks represent larger time intervals. The solid, blue line is the ON-contact threshold (0.08) and dashed, green line is the OFF-contact threshold (0.06).

To ensure good and stable contact, beyond monitoring close proximity to tissue, more criteria are required than a single reflected intensity ratio rising above the threshold to determine ON-contact. These criteria include 5 consecutive readings above the threshold with $< 3\%$ variability between all readings. Figure 5 illustrates the effectiveness of the criteria. In this figure, each of the data points represent the reflected intensity ratio recorded as the probe was placed in contact with tissue in 3 isolated sequences, labeled A-E. Points connected by the dotted line are continuous with a sampling rate of $170ms$, and gaps represent larger time lapses. The

#192160 - $15.00 USD Received 13 Jun 2013; revised 15 Jul 2013; accepted 17 Jul 2013; published 23 Jul 2013

solid, blue line is the ON-contact threshold (0.08) and the dashed, green line is the OFF-contact threshold (0.06). Sequence A represents the probe slowly advancing toward the mucosa, and once in contact with tissue, pressure was continually applied to the probe. Sequence B indicates the probe sliding along the tissue surface. The probe was not held steady and the reflected intensity values are highly variable. In these two sequences, the reflected intensity rises above the threshold, but there is no consistency in the readings. The last sequence (C-E) models the ideal performance where the reflected intensity rises sharply above the threshold (indicating contact with tissue) and maintains a constant value (indicating steadiness of the probe). The 5 points circled in red designate data that meets all criteria for good, stable contact and triggered a tissue measurement. The gap in time sampling immediately following the red circles (approximately $600ms$) is due to the software exiting contact detection mode, entering acquisition mode and re-entering contact detection mode. After data acquisition, the probe is retracted and the reflected intensity drops dramatically below the OFF-contact threshold. We determined 5 consecutive measurements above the threshold provided balance between ensuring contact with tissue and minimizing length of contact time between probe and tissue.

In order to minimize the time it takes to acquire the contact reading, only one collection channel of the probe is acquired. This limits the amount of data to be transferred, as does the number of pixels selected for analysis. We selected only the 10 pixels centered around the optimal wavelength at $525nm$ (average $\sim 3nm$) for evaluation. To further facilitate a rapid detection measurement, the integration time (the amount of time that the spectrometer acquires light for a given measurement) should be as short as possible. A longer integration time provides a higher signal-to-noise ratio, resulting in a larger difference between close proximity with the tissue ($< 2mm$ from tissue surface) and larger distances from the tissue ($> 4mm$ from tissue surface). However, a shorter integration time is desirable to more accurately monitor the probe's change in proximity to tissue. The integration time selected depends on a number of factors, such as the optical fiber parameters, illumination source intensity, tissue type, and the sensitivity of the spectrometers. For our system, an integration time of $20ms$ provides this balance between adequate signal intensity and speed.

As noted earlier in Fig. 2, the length of contact time between the probe and tissue can impact measurements. The current manual, human-initiated triggering is estimated to result in contact times up to 5 seconds or longer. Our aims were consistent timing and automation. Data acquisition is now automatically initiated within 1 second of tissue contact. We determined the time between the start of one contact detection reading and another is approximately $170ms$, and the required 5 consecutive readings take $850ms$ to complete. The software processing can take up to $160ms$ after contact has been confirmed to switch modes for tissue acquisition, but this is negligible compared to previous timing. This timing can be further reduced with different hardware components (such as different spectrometers, communication interfaces, or a control computer) if necessary for a particular application. A significant advantage of implementing this software method is controlled, consistent timing between probe-tissue contact and data acquisition. As processing speeds are increased in our measurement hardware, these data acquisition delays will be decreased.

After tissue contact has been detected, the software exits the contact detection mode, switches to tissue mode, configures the spectrometers for measurements and immediately starts data acquisition to assess the physiological parameters of the tissue. Once acquisition is complete, the software exits tissue mode and re-enters contact detection mode. The software can then automatically detect if the probe is out of contact with the tissue by repeating the process used for ON-contact detection with a modified threshold ratio (or decrease in signal by a predetermined percentage). This threshold is only slightly lower than the ON-contact threshold and requires 2 consecutive readings below the threshold in order to prevent vacillation between detection of

#192160 - $15.00 USD Received 13 Jun 2013; revised 15 Jul 2013; accepted 17 Jul 2013; published 23 Jul 2013

the probe being in contact and out of contact, as well as ensuring the probe is sufficiently out of contact to prevent premature measurements that may be due to poor tissue contact. Once the software process has determined that the probe is sufficiently out of contact from the tissue, the user is informed via an audible and/or visual indicator to again initiate contact with the tissue to acquire another measurement. This automation allows a physician to acquire multiple tissue measurements by simply moving the probe without interaction from other system components (i.e. a triggering button or pedal). The sequence continues until all desired tissue data is collected.

4. Results

Initial in-vivo studies assessed the accuracy of the algorithm to detect both ON-contact and OFF-contact, the reduction in variability of tissue parameters assessed by our fiber-optic probe system and probe-user techniques. The polarization-gated spectroscopy system was used during screening colonoscopy procedures with the probe advanced through the accessory channel. In this study, 2 sets of 10 tissue measurements were taken in the rectum of each patient (n=54). One set of 10 measurements were taken in the 'Manual Mode' which refers to operating the system manually without the algorithm, and another set of 10 measurements taken in the 'Automated Mode' which refers to incorporating the new software method to detect contact and automatically trigger acquisition.

Figure 6 demonstrates the improvement in data quality with the automated algorithm. In Fig. 6(a), the box plot columns represent each physician, grouped by mode, with (+) indicating potential outliers. This figure indicates more variability in data using the 'Manual Mode'. Figure 6(b) shows the variability in measured oxygenation from each physician separately for both inter-patient variability (top panel) and intra-patient (or inter-site) variability (bottom panel). Across all 54 patients, interpatient varaibility decreased from 18% to 12%, and intra-patient variability decreased from 25% to $< 16\%$. Reviewing Fig. 2, we expected an increase in the mean oxygenation between $5-10\%$ since all tissue measurements should start $< 2sec$ after initial contact instead of varying somewhere between $2-10sec$. The mean oxygenation across all patients increased from 54% to 63%. More significantly, using 'Automated mode', the mean oxygenation value for each physician is closer together $(0.604-0.649)$ than data acquired in 'Manual Mode' $(0.483-0.571)$. Also, Physician 'D', whose data did not align with the other 3 physicians, had more consistent data when acquired automatically. Additional tissue parameters, such as hemoglobin concentration, blood vessel radius and total scattering intensity, showed a reduction in variability of only $2-5\%$. This is not surprising because these parameters were not affected by timing as much as oxygenation. These results indicate the potential for optimization of the algorithm to improve the data quality, repeatability and consistency.

To evaluate the accuracy of the automated algorithm to detect contact, we monitored the change in probe position from the colon mucosa on the endoscope camera and documented whether the algorithm accurately detected when the probe was 'ON' and 'OFF' contact with the tissue. For ON-contact, the algorithm accurately detected contact and triggered 91% of tissue measurements. In 8% of the failed detection cases, the reflected intensity was below the threshold and the remaining 1% either saturated the detector or failed for unknown reasons. There were additional cases when the probe was in contact and no data acquired, but these corresponded to high variability in reflected intensity (similar to case A and B in Fig. 5). Thus, the algorithm accurately detected the probe movement and this 4% of the data was not included as measurements that failed to trigger. For OFF-contact, the accuracy was 83%, with 11% of failures related to contamination on the probe tip (i.e. stool) and 6% of failures not falling below the threshold when the probe was removed from contact. If contamination occurred during tissue contact, the probe tip was rinsed with water (i.e. flush cleaned) to remove the

#192160 - $15.00 USD Received 13 Jun 2013; revised 15 Jul 2013; accepted 17 Jul 2013; published 23 Jul 2013

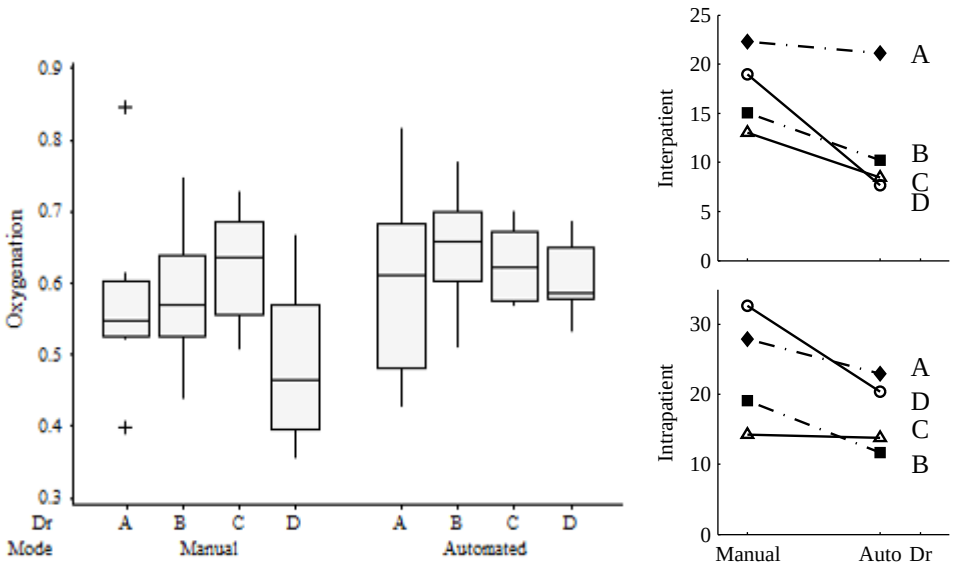

(a) Mean Oxygenation grouped by physician

(b) Variability (%)

Fig. 6. Initial in-vivo evaluation of automated algorithm across physicians. (a) Mean oxygenation per patient is grouped by physician for both modes of data acquisition. Data acquired with the 'Automated Mode' show reduction in the spread of oxygenation values, fewer outliers (denoted as +) and the mean value for each physician is more closely matched ($0.604 - 0.649$) than data acquired in the 'Manual Mode'($0.483 - 0.571$). Also, the 'Auto Mode' reduces both the Interpatient variability ((b) top panel) and the Intrapatient variability ((b) bottom panel).

contaminate allowing the algorithm to detect OFF-contact.

5. Discussion

We leveraged the nature of our fiber-optic probe system to develop an optical method of detecting contact with tissue. This only required a software algorithm to configure the current components of our device (i.e. spectrometers) and analyze reflected light. The intensity of reflected light is related to the probe distance from tissue surface (Fig. 4) which would make this design akin to an optical proximity sensor. The additional requirement of consecutive readings within a defined limit of one another effectively make this method a contact sensor. This is an important distinction since probe-tissue contact is a requirement for data quality. The criteria to define an optimal wavelength, integration time and additional parameters were presented so that it can easily be integrated into any other fiber-optic probe system in biomedical applications.

The greatest advantage of incorporating this method into a fiber-optic probe device is the ability to initiate a single or multiple tissue measurements automatically once contact is detected. The physician can simply advance the probe toward the target tissue, use their haptic perception to feel for contact while the software algorithm confirms contact and communicates the result via an audible tone (beep). Then, by removing the probe from the tissue surface for a brief moment ($< 1sec$) and placing it back in contact, a new tissue measurement can be acquired. This removes interfacing with a data recording device or using an external trigger (i.e. button or pedal) during the probe manipulation and allows the entire focus to stay on the proce-

#192160 - $15.00 USD Received 13 Jun 2013; revised 15 Jul 2013; accepted 17 Jul 2013; published 23 Jul 2013

dure. This feature can expand data acquisition in applications with limited or no visualization of the target tissue.

Fiber-optic probe technologies have shown promise in an endoscopic setting [6, 21]. However, for these technologies to truly be used as a screening tool and have an impact on the broader population, they need to be used in the primary care office setting. In the case of colon cancer screening, a primary care physician would need to take rectal measurements and this requires blind insertion of the probe where the automated algorithm would ensure accurate data acquisition. We initiated a pilot study using this method with a blind insertion protocol of another probe technology from our group, described in Ref. [22]. This protocol is similar to the methods outlined in this paper (10 'Manual' and 10 'Automated' mode measurements), except the probe is 'blindly' inserted into the rectum prior to a colonoscopy without the use of an endoscope. In the three patients recruited thus far, the inter-patient variability was reduced from 25% to 18%; and the intra-patient variability was reduced from 15% to 7%. We are continuing to test the performance of this algorithm on a larger scale with this blind protocol, and plan to extend the study into the clinical setting on patients who have not completed bowel preparation. The algorithm performance remained the same with 92% accuracy for ON-contact detection and 80% accuracy for OFF. Further analysis should also review the thresholds in order to make them more robust and increase the accuracy of both 'ON' and 'OFF'-contact detection.

In addition to facilitating the use of these technologies during procedures, this software method can improve data quality and reduce variability. Variability results from several factors, including biological (i.e. interpatient), systematic (i.e. light source, probes, and timing), and user techniques (i.e. pressure and length of contact). System differences and user techniques were discussed earlier and potentially alter physiological measurements from the tissue which can impact the classification accuracy in diagnostic applications. An automated contact detection with controlled timing reduces some of this variability through minimizing any time delays between probe-tissue contact and data acquisition. One example, reported above, was a decrease in oxygenation as the length of contact time increased between the probe and tissue. As we expected, the reliable detection of the algorithm and consistent timing from detection to trigger resulted in higher oxygenation values compared to the manual mode. Although this design cannot measure pressure, the use of a consistent time frame partially alleviates this limitation. We use an audible cue to inform the physician that contact has been detected and a tissue measurement has started. The idea is this feedback prevents the physician from continuing to apply pressure. Our initial in-vivo data indicates lower variability in the measurements within a patient and across all patients in the study. This gives us confidence that we can address the impact of pressure without directly measuring or controlling pressure applied to the probe. Lastly, each physician develops their own style and technique when using medical instruments and this was quantified as a source of variability in one study evaluating the repeatability of fluorescence spectroscopy for cervical neoplasia [23]. In our study, the increase in mean oxygenation of each physician represents an improvement in data quality as the contact algorithm can reduce variability from pressure, steadiness of the hand, long contact times or possible bias from years of experience. This highlights the potential for this automated method to serve as a training tool for physicians using fiber-optic probes in a research setting, and ultimately as a clinical device. For example, the physicians can use the contact detection algorithm together with a real time graph of the reflected intensity readings (similar to Fig. 5 and already displayed on our devices) to increase their haptic perception of the tissue surface while placing the probe in contact, and to monitor the steadiness of their hand while maintaining contact with tissue. We expect the performance to improve with additional use and will re-evaluate once we acquire more data using the automated method.

#192160 - $15.00 USD Received 13 Jun 2013; revised 15 Jul 2013; accepted 17 Jul 2013; published 23 Jul 2013

6. Conclusion

In this paper, a novel software method is proposed that can be incorporated into current fiber-optic probe systems without additional hardware. We presented the criteria that can be modified to the sensitivity of different spectrometers, transmission properties of different fibers, alternate probe geometries/designs or different tissue properties. We are not aware of another method that uses a similar approach to provide proximity or contact feedback without hardware modification. Most importantly, the automated algorithm reduced the variability of in-vivo data, especially related to individual physicians. Some sources of variability impact classification of data and this algorithm could potentially improve diagnostic performance. Additionally, the automation of detecting contact provides a vast improvement in the ease of acquiring data from tissue since the interaction of the physician is focused on the movement of the probe and no longer requires direct visualization or involves interfacing with an external trigger (i.e. a button or pedal) during the probe manipulation. This technology has the ability to expand the biomedical applications and increase the robustness of fiber-optic probe systems.

Acknowledgments

This study was funded by Northwestern University and the NIH (grant nos. R01CA128641, R01EB003682, R01CA109861, and F31CA144561)

#192160 - $15.00 USD Received 13 Jun 2013; revised 15 Jul 2013; accepted 17 Jul 2013; published 23 Jul 2013